PHYSICS RESULTS FROM THE ARGO-YBJ EXPERIMENT

GIUSEPPE DI SCIASCIO
ON BEHALF OF THE ARGO-YBJ COLLABORATION

INFN, Sez. Roma TorVergata
Via della Ricerca Scientifica 1, I-00133 Roma, Italy

Abstract

The ARGO-YBJ experiment has been in stable data taking since November 2007 at the YangBaJing Cosmic Ray Laboratory (Tibet, P.R. China, 4300 m a.s.l.). In this paper we report a few selected results in Gamma-Ray Astronomy (Crab Nebula and Mrk421 observations, search for high energy tails of GRBs) and Cosmic Ray Physics (Moon and Sun shadow observations, proton-air cross section and $\overline{p}$/p preliminary measurements).

1 The detector

The ARGO-YBJ experiment, located at the YangBaJing Cosmic Ray Laboratory (Tibet, P.R. China, 4300 m a.s.l.), is an air shower array exploiting the full coverage approach at very high altitude, with the aim of studying the cosmic radiation with a low energy threshold (a few hundreds of GeV). The detector is constituted by a central carpet, made of a single layer of Resistive Plate Chambers (RPCs) with ∼92% of active area, enclosed by a guard ring partially instrumented (∼40%) mainly to improve the rejection capability for external events. The apparatus has a modular structure, the basic element being a cluster (5.7×7.6 m^2), divided into 12 RPCs (2.8×1.25 m^2 each). Each chamber is read by 80 strips of 6.75×61.8 cm^2 (the spatial pixel), logically organized in 10 independent pads of 55.6×61.8 cm^2 which are individually acquired and represent the time pixel of the detector. In order to extend the dynamic range up to PeV energies, a charge read-out has been implemented by instrumenting every RPC also with two large size pads of dimension 140×125 cm^2 each. The full detector is composed of 154 clusters for a total active surface of $\sim$6700 m^2 (Aielli G. et al., 2006). A 0.5 cm thick lead converter will cover the apparatus uniformly in order to improve the angular resolution at lower energies.

The detector is connected to two different data acquisition systems, working independently, and corresponding to the two operation modes, shower and scaler. In shower mode, for each event the location and timing of every detected particle is recorded, allowing the lateral distribution and arrival direction reconstruction (Di Sciascio G. et al., 2007). In scaler mode the total counts are measured every 0.5 s, with very poor information on both the space distribution and arrival direction of the detected particles. For each cluster, the signal coming from the 120 pads is added up and put in coincidence in a narrow time window (150 ns), giving the counting rates of $\geq$1, $\geq$2, $\geq$3, $\geq$4 pads, that are read by four independent scaler channels. The corresponding measured rates are, respectively, $\sim$40 kHz, $\sim$2 kHz, $\sim$300 Hz and $\sim$120 Hz for each cluster (Aielli G. et al., 2008).

Since 2007 November the detector has been in stable data taking with a multiplicity trigger $N_{pad} \geq 20$ and a duty cycle $\geq$ 85%: the trigger rate is about 3.5 kHz. In this paper we report on the first results in Gamma-Ray Astronomy and Cosmic Ray Physics.

2 Gamma-Ray Astronomy

In this analysis all events are considered, without any internal shower selection. No lead converter has been mounted on the RPCs yet (with the lead we expect an improvement of the angular resolution and, consequently, of the sensitivity, of $\approx$40% at TeV energies). The cosmic ray background rejection is performed by exploiting the good angular resolution of the detector and the fact that at this altitude the trigger efficiency of TeV γ-rays is $\approx$2 times larger than that of protons at fixed energy. No additional γ/hadron discrimination algorithms have been yet applied. We expect an improvement of our sensitivity of a factor $\approx$1.5 by applying "topological" selection

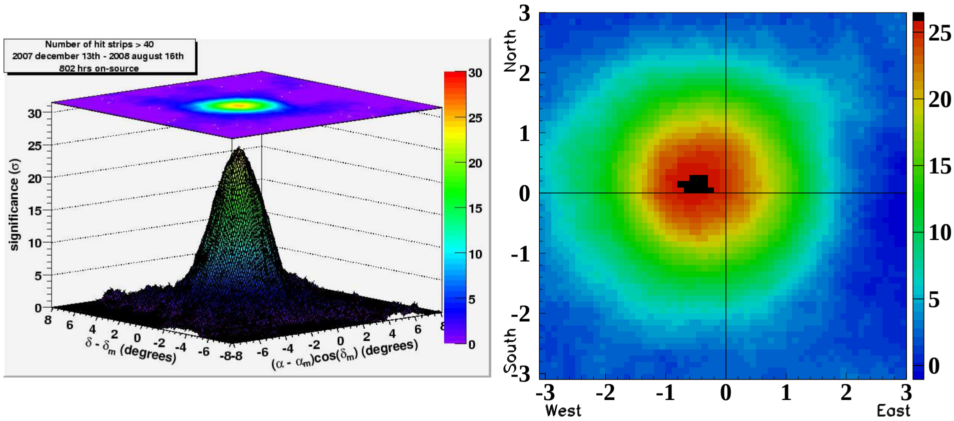

Figure 1: Point Spread Function of the ARGO-YBJ detector around the Moon observed in 2008 for showers with N_{pad} ≥40 (left plot). In the right plot the corresponding Moon shadow significance map is shown. The color scale gives the significance.

criteria presently under study (Dattoli M. et al., 2007).

2.1 Angular Resolution

We have measured the pointing accuracy of the ARGO-YBJ detector by studying the Moon shadow. Cosmic rays are hampered by the Moon, therefore a deficit of cosmic rays in its direction is expected (the so-called "Moon shadow"). The Moon shadow is an important tool to calibrate the performance of an air shower array. In fact, the size of the deficit allows a measurement of the angular resolution and the position of the deficit allows the evaluation of the absolute pointing accuracy of the detector. In addition, positively charged particles are deflected towards East due to the geomagnetic field by an angle $\Delta\theta \sim 1.6°/E(TeV)$. Therefore, the observation of the displacement of the Moon provides a direct check of the relation between shower size and primary energy thus calibrating the detector.

The ARGO-YBJ experiment is observing the Moon shadow with a sensitivity of about 10 standard deviations per month at a multiplicity N_{pad} ≥40, with the zenith angle $\theta < 50°$ (corresponding to a proton median energy E_{50} ≈1.8 TeV). In Fig.1 the shadow observed in the period December 2007 - August 2008 (802 hours on-source) is shown. In the left plot the 3D view of the shadow (i.e., the Point Spread Function of the detector) is shown. The

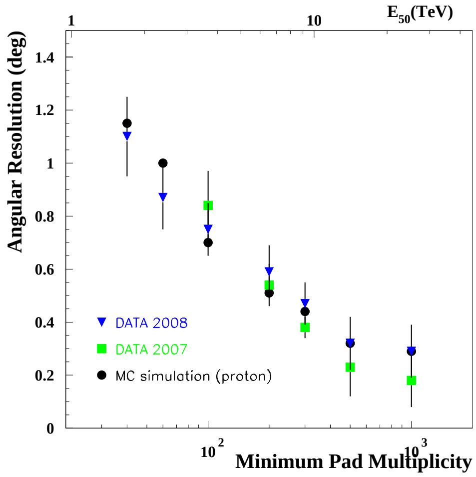

Figure 2: Measured angular resolution compared with MC simulations as a function of pad multiplicity.

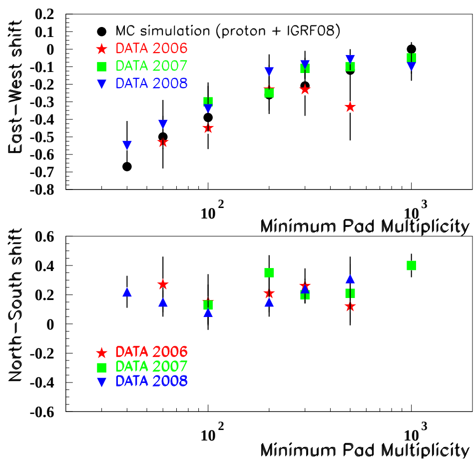

Figure 3: Displacement of the Moon shadow in the East-West (upper panel) and North-South (lower panel) directions as a function of pad multiplicity.

sensitivity of the observation is about 26 standard deviations as can be seen from the Moon shadow map in the right plot of Fig.1. In Fig.2 the angular resolution measured with the Moon shadow method in 2007 and 2008 is compared to MC simulation. The upper scale refers to the median energy of the triggered protons. As can be seen, the values are in fair agreement: the angular resolution of the ARGO-YBJ experiment is less than 0.6° for $N_{pad} \geq 200$ ($E_{50} \approx 6$ TeV). In Fig.3 the displacements of the Moon shadow in the East-West (upper panel) and North-South (lower panel) directions are shown. In the upper figure the measured shift towards West due to the geomagnetic field is compared to a MC simulation of the proton propagation in Earth-Moon system. As can be seen, the fair agreement between the measurements and the simulations make us confident about the energy calibration of the detector. The study of the displacement along the North-South axis, not affected by the geomagnetic field at the Yangbajing site, enables us to estimate the magnitude of the systematic pointing error without the Moon shadow simulation. From this preliminary analysis it results that there is a residual systematic shift towards North of ≈0.2°, less than the angular resolution. Deeper analysis is in progress in order to eliminate this pointing error. I would like to emphasize that these results are stable even

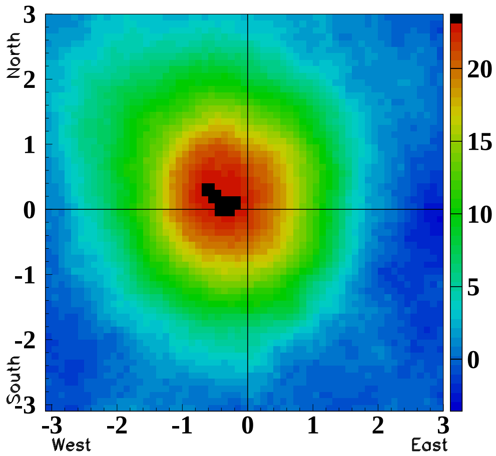

Figure 4: Shadow of the Sun observed from December 2007 to August 2008.

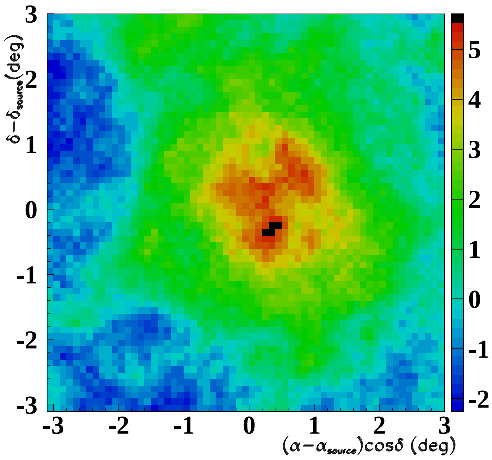

Figure 5: Significance map of the Crab Nebula region observed from January to August 2008.

in periods mainly devoted to installation and debugging operations (2006 and 2007). This makes us confident about the stability of the detector.

The shadow of the Sun measured in the period December 2007 - August 2008 (954 hours on-source with $\theta < 50°$) for events with $N_{pad} \geq 40$ is shown in Fig. 4. The significance of the maximum event deficit is about 25σ: the shadow is well visible, as expected near the solar minimum. The displacement of the shadow from the apparent position of the Sun could be explained by the effect of the geomagnetic field and of the solar and Interplanetary Magnetic Fields (IMF) whose configuration considerably changes with the phases of the solar activity cycle (Amenomori M. et al., 2000). Therefore, high energy cosmic rays may bring direct information on the structure of the IMF under the influence of the solar activity. This result shows the capability of the ARGO-YBJ experiment to study the effect of the IMF on the Sun shadow down to the TeV energy region with a monthly recurrence.

2.2 Gamma Ray Sources

Fig.5 shows the significance map of the Crab Nebula region measured with the full ARGO-YBJ detector during days 1-229 of 2008 (1143 hours on-source with $\theta < 40°$) with a multiplicity $N_{pad} \geq 40$, corresponding to a photon median energy of about 1 TeV (E_{mode} ∼0.4 TeV). As can be seen from the map a clear signal is evident at a level of about 6 standard deviations. Deeper analysis and further data integration are in progress in order to evaluate the final sensitivity of the detector. Nevertheless, we note that this is the first time that an air shower array is able to detect photons from a point source with such a low peak energy.

The detector started recording data with the full central carpet during the X-ray flare of Mrk421 in July 2006. The ARGO-YBJ experiment observed this source in the days 190 - 245 (109 hours on-source) with a multiplicity N_{pad} ≥60. A clear evidence of a TeV emission at a level of about 6 standard deviations was observed. The detector was in its commissioning phase, therefore new analysis are in progress to properly evaluate the statistical significance of the observation.

Mrk421 was again flaring during the first months of 2008 and the ARGO-YBJ experiment again reported evidence for a TeV emission in correlation with the X-ray flares. The significance map of the Mrk421 region is shown in Fig.6: a clear signal at about 7 standard deviations level is visible during the 2008 (days 1 - 229, 1217 hours on-source). The observation refers to a multiplicity N_{pad} ≥60. A correlation of TeV photons detected by the ARGO-YBJ experiment with the X-ray events detected by the Rossi RXTE Satellite is evident in Fig. 7 for two different multiplicity values.

We note that an all-sky VHE gamma-ray telescope as the ARGO-YBJ experiment is able to monitor the Mrk421 in a continuous way, not being affected by the problems of the Cherenkov telescopes which can operate only on clear moonless nights.

2.3 Search for GRBs with the Scaler Mode

The Scaler Mode technique offers a unique tool to study GRBs in the GeV energy range, where γ-rays are less affected by the absorption due to pair production in the extragalactic space. In order to extract the maximum information from the data, several GRB searches have been implemented: (1) search in coincidence with the satellite detection; (2) search for a delayed or anticipated signal of fixed duration; (3) phase pile-up of all GRBs. The search has been done in coincidence with 38 GRBs observed by satellites (mainly SWIFT) in the period December 2004 - March 2008 in the ARGO-YBJ field of view ($\theta < 45°$). No deviation from the statistical behaviour has been found either in coincidence with the low energy detection, or in an interval of 2 hours around it (Di Girolamo T. et al., 2007). The correspond-

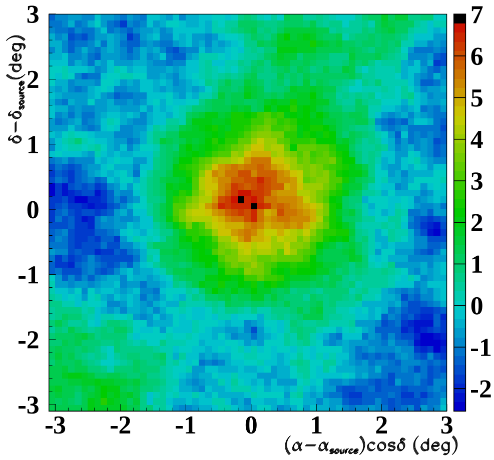

Figure 6: Significance map of the Mrk421 region observed up to August 2008.

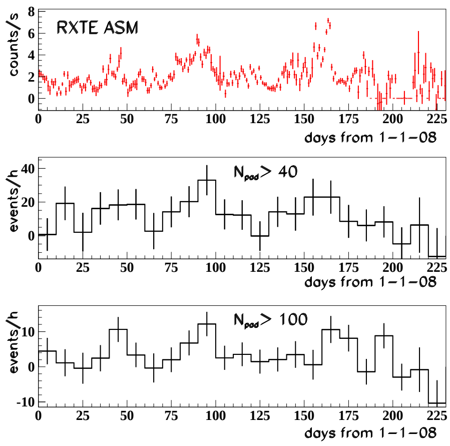

Figure 7: Correlation between X-ray data and TeV photons for two multiplicity values.

ing upper limits on the fluence are of the order of 10^{-6} - 10^{-4} erg/cm^2 in the 1 - 100 GeV range, well below the energy range explored by the present generation of Cherenkov telescopes.

3 Cosmic Ray Physics

3.1 Measurement of the Proton-Air Cross Section

A preliminary measurement of the proton-air cross section has been performed by exploiting the attenuation of cosmic ray flux with increasing zenith angles θ (i.e., atmospheric depths) $\propto$ exp(-$x_0\cdot$ (secθ-1)/Λ_{obs}), where x_0 is the vertical atmospheric depth of the detector and Λ_{obs} is the observed attenuation length of air showers, related to the mean free path λ_{int} of the primary through the parameter K=$\Lambda_{obs}/\lambda_{int}$. Therefore, with a measurement of the attenuation length we can estimate, in principle, the p-air and p-p cross sections. The K parameter, which takes into account the fluctuations both in the shower development and in the shower sampling, is calculated via MC simulation. The analysis has been performed in two multiplicity bins, 300$\leq$$N_{pad}$ $\leq$1000 and N_{pad} >1000, corresponding to mean energies (3.9$\pm$0.1) TeV and (12.7$\pm$0.4) TeV, respectively. The measured

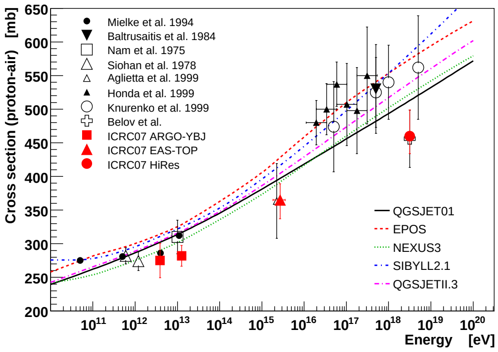

Figure 8: Current data of proton-air production cross section measurements.

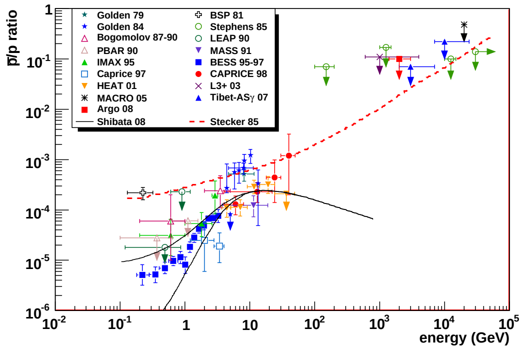

Figure 9: Status of the measurements of the $\overline{p}/p$ ratio.

p-air cross section values are (275±51) mb and (282±31) mb, respectively (De Mitri I. et al., 2007) (see Fig.8). Further studies are in progress in order to extend the measurement to the PeV energy region.

3.2 Measurement of the antiproton/proton ratio

In order to measure the $\overline{p}/p$ ratio at TeV energies we exploit the Earth-Moon system as an ion spectrometer: if protons are deflected towards East, antiprotons are deflected towards West. If the energy is low enough and the angular resolution small we can distinguish, in principle, between two shadows, one shifted towards West due to the protons and the other shifted towards East due to the antiprotons. If no event deficit is observed on the antimatter side an upper limit on the antiproton content can be calculated. A very preliminary measurement has been performed with the ARGO-YBJ experiment for $N_{pad} \geq 40$ in the period December 2007 - August 2008 (802 hours on-source). For this multiplicity the Moon shadow shifts westward by about 0.45°, at a median energy ≈2 TeV (mode energy ≈0.5 TeV). The data is in fair agreement with MC simulation. The deficit events around the Moon shadow are fitted with a Gaussian formula: protons are estimated to be ∼70% of cosmic rays. A preliminary upper limit on the antiproton/proton ratio at the 90% confidence level is calculated to be about 10% and reported in Fig. 9 which shows the status of the antiproton/proton measurements. We note that in the multi-TeV range this result is among the lowest available.

References

[1] Aielli G. at al.: 2006, *NIM* **A562**, 92.

[2] Aielli G. et al.: 2008, *Astrop. Phys.* **30**, 85.

[3] Amenomori M. at al.: 2000, *ApJ* **541**, 1051.

[4] Dattoli M. et al.: 2007 in Proc. *30th ICRC*, in press.

[5] De Mitri I. et al.: 2007 in Proc. *30th ICRC*, in press.

[6] Di Girolamo T. et al.: 2007 in Proc. *30th ICRC*, in press.

[7] Di Sciascio G. et al.: 2007 in Proc. *30th ICRC*, in press.

DISCUSSION

A. SANTANGELO: In the plots of the Crab appears that a smaller significance is obtained with a longer exposure time. Can you tell us why?

G. DI SCIASCIO: The statistical significance of the 2008 Crab observation appears smaller than that of 2007. This may have been caused by a statistical signal fluctuation: the 2007 data sample is about a factor of 5 smaller than that integrated up to August 2008. Nevertheless this analysis is yet preliminary and deeper reanalysis is in progress in order to evaluate the final sensitivity of the detector properly.